Editors' Suggestion

Inferring the Dynamics of Underdamped Stochastic Systems

David B. Brückner,[1,†] Pierre Ronceray,[2,†] and Chase P. Broedersz[1,3,*]

[1]Arnold Sommerfeld Center for Theoretical Physics and Center for NanoScience, Department of Physics, Ludwig-Maximilian-University Munich, Theresienstr. 37, D-80333 Munich, Germany

[2]Center for the Physics of Biological Function, Princeton University, Princeton, New Jersey 08544, USA

[3]Department of Physics and Astronomy, Vrije Universiteit Amsterdam, 1081 HV Amsterdam, The Netherlands

(Received 14 February 2020; revised 26 April 2020; accepted 24 June 2020; published 29 July 2020)

Many complex systems, ranging from migrating cells to animal groups, exhibit stochastic dynamics described by the underdamped Langevin equation. Inferring such an equation of motion from experimental data can provide profound insight into the physical laws governing the system. Here, we derive a principled framework to infer the dynamics of underdamped stochastic systems from realistic experimental trajectories, sampled at discrete times and subject to measurement errors. This framework yields an operational method, Underdamped Langevin Inference, which performs well on experimental trajectories of single migrating cells and in complex high-dimensional systems, including flocks with Viscek-like alignment interactions. Our method is robust to experimental measurement errors, and includes a self-consistent estimate of the inference error.

DOI: 10.1103/PhysRevLett.125.058103

Across the scientific disciplines, data-driven methods are used to unravel the dynamics of complex systems. These approaches often take the form of inverse problems, aiming to infer the underlying governing equation of motion from observed trajectories. This problem is well understood for deterministic systems [1–3]. For a broad variety of physical systems, however, a deterministic description is insufficient: fast, unobserved degrees of freedom act as an effective dynamical noise on the observable quantities. Such systems are described by Langevin dynamics, and inferring their equation of motion is notoriously harder: one must then disentangle the stochastic from the deterministic contributions, both of which contribute to shape the trajectory. In molecular-scale systems described by the overdamped Langevin equation, a first-order stochastic differential equation, recently developed techniques make it possible to efficiently reconstruct the dynamics from observed trajectories [4–8]. Many complex systems at larger scales, however, exhibit stochastic dynamics governed by the underdamped Langevin equation, a second-order stochastic differential equation. Examples include cell motility [9–13], postural dynamics in animals [14,15], movement in interacting swarms of fish [16–18], birds [19,20], and insects [21,22], as well as dust particles in a plasma [23]. Due to recent advances in tracking technology, the diversity, accuracy, dimensionality, and size of these behavioral datasets is rapidly increasing [24], resulting in a growing need for accurate inference approaches for high-dimensional underdamped stochastic systems. However, there is currently no rigorous method to infer the dynamics of such underdamped stochastic systems.

Inference from underdamped stochastic systems suffers from a major challenge absent in the overdamped case. In any realistic application, the accelerations of the degrees of freedom must be obtained as discrete second derivatives from the observed position trajectories, which are sampled at discrete intervals Δt. Consequently, a straightforward generalization of the estimators for the force and noise fields of overdamped systems fails: these estimators do not converge to the correct values, even in the limit $\Delta t \to 0$ [25,26]. To make matters worse, real data is always subject to measurement errors, leading to divergent biases in the discrete estimators [27]. These problems have so far precluded reliable inference in underdamped stochastic systems.

Here, we introduce a general framework, Underdamped Langevin Inference (ULI), that conceptually explains the origin of these biases, and provides an operational scheme to reliably infer the equation of motion of underdamped stochastic systems governed by nonlinear force fields and multiplicative noise amplitudes. To provide a method that can be robustly applied to realistic experimental data, we rigorously derive estimators that converge to the correct values for discrete data subject to measurement errors. We demonstrate the power of our method by applying it to experimental trajectories of single migrating cells, as well as simulated complex high-dimensional data sets, including flocks of active particles with Viscek-style alignment interactions.

We consider a general d-dimensional stationary stochastic process $\mathbf{x}(t)$ with components $\{x_\mu(t)\}_{1\le\mu\le d}$ governed by the underdamped Langevin equation

$$\dot{x}_\mu = v_\mu,$$
$$\dot{v}_\mu = F_\mu(\mathbf{x},\mathbf{v}) + \sigma_{\mu\nu}(\mathbf{x},\mathbf{v})\xi_\nu(t), \quad (1)$$

which we interpret in the Itô sense. Throughout, we employ the Einstein summation convention, and $\xi_\mu(t)$ represents a Gaussian white noise with the properties $\langle \xi_\mu(t)\xi_\nu(t')\rangle = \delta_{\mu\nu}\delta(t-t')$ and $\langle \xi_\mu(t)\rangle = 0$. Our aim is to infer the force field $F_\mu(\mathbf{x},\mathbf{v})$ and the noise amplitude $\sigma_{\mu\nu}(\mathbf{x},\mathbf{v})$ from an observed finite trajectory of the process [28].

We start by approximating the force field as a linear combination of n_b basis functions $b = \{b_\alpha(\mathbf{x},\mathbf{v})\}_{1\le\alpha\le n_b}$, such as polynomials, Fourier modes, wavelet functions, or Gaussian kernels [14]. From these basis functions, we construct an empirical orthonormal basis $\hat{c}_\alpha(\mathbf{x},\mathbf{v}) = \hat{B}^{-1/2}_{\alpha\beta} b_\beta(\mathbf{x},\mathbf{v})$ such that $\langle \hat{c}_\alpha \hat{c}_\beta\rangle = \delta_{\alpha\beta}$, an approach that was recently proposed for overdamped systems [8]. Here and throughout, averages correspond to time averages along the trajectory. We can then approximate the force field as $F_\mu(\mathbf{x},\mathbf{v}) \approx F_{\mu\alpha}\hat{c}_\alpha(\mathbf{x},\mathbf{v})$. Similarly, we perform a basis expansion of the noise amplitude $\sigma^2_{\mu\nu}(\mathbf{x},\mathbf{v})$. Thus, the inference problem reduces to estimating the projection coefficients $F_{\mu\alpha}$ and $\sigma^2_{\mu\nu\alpha}$.

Dealing with discreteness.—In practice, only the configurational coordinate $\mathbf{x}(t)$ is accessible in experimental data, sampled at a discrete time interval Δt. We therefore only have access to the discrete estimators of the velocity $\hat{\mathbf{v}}(t) = [\mathbf{x}(t) - \mathbf{x}(t-\Delta t)]/\Delta t$ and acceleration $\hat{\mathbf{a}}(t) = [\mathbf{x}(t+\Delta t) - 2\mathbf{x}(t) + \mathbf{x}(t-\Delta t)]/\Delta t^2$. Our goal is to derive an estimator $\hat{F}_{\mu\alpha}$, constructed from the discrete velocities and accelerations, which converges to the exact projections $F_{\mu\alpha}$ in the limit $\Delta t \to 0$.

An intuitive approach would be to simply generalize the estimators for overdamped systems [8] and calculate the projections of the accelerations $\langle \hat{a}_\mu \hat{c}_\alpha(\mathbf{x},\hat{\mathbf{v}})\rangle$. This expression has indeed previously been used for underdamped systems [13,14,25,27]. We derive the correction term to this estimator by expanding the basis functions $\hat{c}_\alpha(\mathbf{x},\hat{\mathbf{v}}) = \hat{c}_\alpha(\mathbf{x},\mathbf{v}) + (\partial_{v_\mu}\hat{c}_\alpha)(\hat{v}_\mu - v_\mu) + \ldots$, where the leading order contribution to the second term is a fluctuating (zero average) term of order $\Delta t^{1/2}$. Similarly, we perform a stochastic Itô-Taylor expansion of the discrete acceleration $\hat{\mathbf{a}}(t)$, which has a leading order fluctuating term of order $\Delta t^{-1/2}$ [29]. Thus, while each of these terms individually averages to zero, their product results in a bias term with nonzero average of order Δt^0: $\langle \hat{a}_\mu \hat{c}_\alpha(\mathbf{x},\hat{\mathbf{v}})\rangle = F_{\mu\alpha} + \frac{1}{6}\langle \sigma^2_{\mu\nu}\partial_{v_\nu}\hat{c}_\alpha(\mathbf{x},\mathbf{v})\rangle + \mathcal{O}(\Delta t)$ [30]. As expected, this bias vanishes in the limit $\sigma \to 0$, and therefore does not appear in deterministic systems. However, it poses a problem wherever a second derivative of a stochastic signal is averaged conditioned on its first derivative. The occurrence of such a bias was observed in linear systems [25,26]. Specifically, for a linear viscous force $F(v) = -\gamma v$, it was found that $\langle \hat{a}\,\hat{c}(\hat{v})\rangle = -\frac{2}{3}\gamma + \mathcal{O}(\Delta t)$, which is recovered by our general expression for the systematic bias [30].

Previous approaches to correct for this bias rely on *a priori* knowledge of the observed stochastic process [25], are limited to simple parametric forms [26], or perform an *a posteriori* empirical iterative scheme [13]. In contrast, by simply deducting the general form of the bias, we obtain our ULI estimator [30]:

$$\hat{F}_{\mu\alpha} = \langle \hat{a}_\mu \hat{c}_\alpha(\mathbf{x},\hat{\mathbf{v}})\rangle - \frac{1}{6}\langle \widehat{\sigma^2}_{\mu\nu}(\mathbf{x},\hat{\mathbf{v}})\partial_{v_\nu}\hat{c}_\alpha(\mathbf{x},\hat{\mathbf{v}})\rangle \quad (2)$$

The presence of the derivative of a basis function in the estimator highlights the importance of projecting the dynamics of underdamped systems onto a set of *smooth* basis functions, in contrast to the traditional approach of taking conditional averages in a discrete set of bins [4,5], equivalent to a basis of nondifferentiable top-hat functions.

Similarly to the force field, we expand the noise amplitude as a sum of basis functions, and derive an unbiased estimator for the projection coefficients [30]

$$\widehat{\sigma^2}_{\mu\nu\alpha} = \frac{3\Delta t}{2}\langle \hat{a}_\mu \hat{a}_\nu \hat{c}_\alpha(\mathbf{x},\hat{\mathbf{v}})\rangle \quad (3)$$

To test our method, we start with a simulated minimal example, the stochastic damped harmonic oscillator $\dot{v} = -\gamma v - kx + \sigma\xi$ [Figs. 1(a)–(e)]. Indeed, we find that even for such a simple system, the intuitive acceleration projections $\langle \hat{a}_\mu \hat{c}_\alpha(\mathbf{x},\hat{\mathbf{v}})\rangle$ yield a biased result [Fig. 1(e)]. In contrast, ULI, defined by Eqs. (3) and (2), provides an accurate reconstruction of the force field [Figs. 1(c) and 1(e)]. To test the convergence of these estimators in a quantitative way, we calculate the expected random error due to the finite length τ of the input trajectory, $\delta\hat{F}^2/\hat{F}^2 \sim N_b/2\hat{I}_b$, where we define $\hat{I}_b = (\tau/2)\hat{\sigma}^{-2}_{\mu\nu}\hat{F}_{\mu\alpha}\hat{F}_{\nu\alpha}$ as the empirical estimate of the information contained in the trajectory, and $N_b = dn_b$ is the number of degrees of freedom in the force field [8]. We confirm that the convergence of our estimators follows this expected trend, in contrast to the biased acceleration projections [Fig. 1(d)]. Therefore, ULI provides an operational method to accurately infer the dynamical terms of underdamped stochastic trajectories.

Treatment of measurement errors.—A key challenge in stochastic inference from real data is the unavoidable presence of time-uncorrelated random measurement errors $\boldsymbol{\eta}(t)$, which can be non-Gaussian: the observed signal in this case is $\mathbf{y}(t) = \mathbf{x}(t) + \boldsymbol{\eta}(t)$. This problem is particularly dominant in underdamped inference, where the signal is differentiated twice, leading to a divergent bias of order Δt^{-3} [30]. Thus, for small Δt, even small measurement errors can lead to prohibitively large systematic inference errors, which cannot be rectified by simply recording more data.

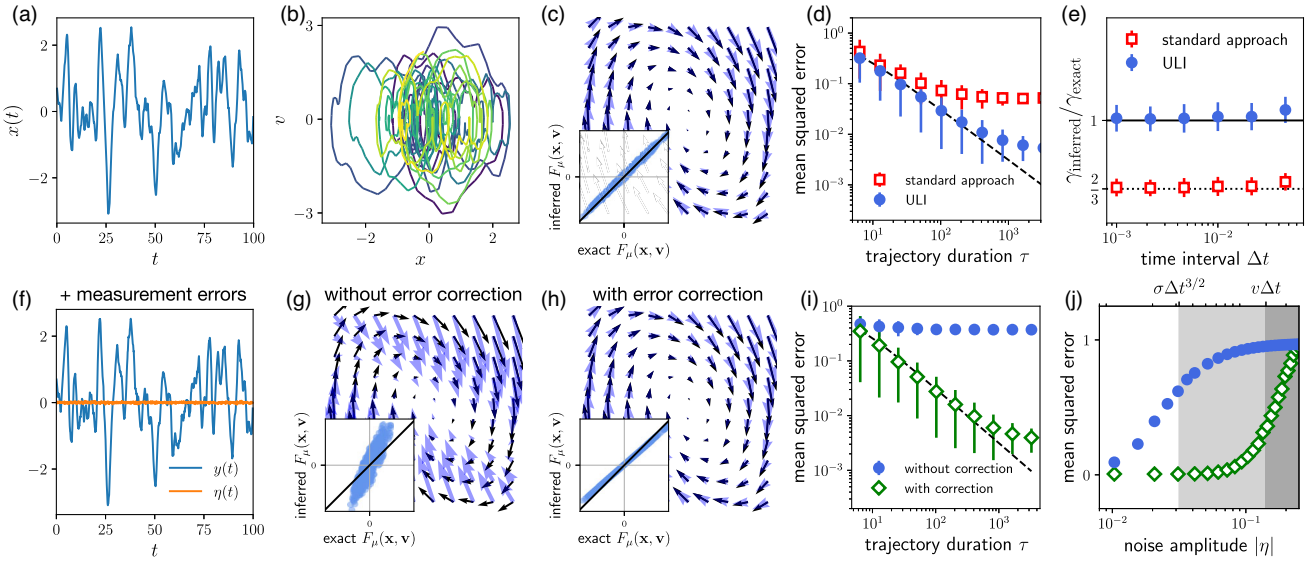

FIG. 1. Inference from discrete time series subject to measurement error. (a) Trajectory $x(t)$ of a stochastic damped harmonic oscillator, $F(x,v) = -\gamma v - kx$. (b) The same trajectory represented in xv-phase space. Color coding indicates time. (c) Force field in xv-space inferred from the trajectory in (a) using ULI with basis functions $b = \{1, x, v\}$ (blue arrows), compared to the exact force field (black arrows). Inset: inferred components of the force along the trajectory versus the exact values. (d) Convergence of the mean squared error of the inferred force field, obtained using ULI (circles) and with the previous standard approach [13,14,25,27] (squares). Dashed lines indicate the predicted error $\delta\hat{F}^2/\hat{F}^2 \sim N_b/2\hat{I}_b$. (e) Inferred friction coefficient γ divided by the exact one as a function of the sampling time interval Δt, comparing the previous standard approach to ULI. (f) Trajectory $y(t) = x(t) + \eta(t)$ (blue) corresponding to the same realization $x(t)$ in (a), with additional time-uncorrelated measurement error $\eta(t)$ (orange) with small amplitude $|\eta| = 0.02$. (g), (h) Force field inferred from $y(t)$ using estimators without and with measurement error corrections, respectively. (i) Inference convergence for data subject to measurement error using estimators without (circles) and with (diamonds) measurement error corrections. (j) Dependence of the inference error on the noise amplitude $|\eta|$ [same symbols as in (i)].

To overcome this challenge, we derive estimators which are robust against measurement error. These estimators are constructed such that the leading-order bias terms cancel. For the force estimator, we find that this is achieved by using the local average position $\bar{\mathbf{x}}(t) = \frac{1}{3}[\mathbf{x}(t-\Delta t) + \mathbf{x}(t) + \mathbf{x}(t+\Delta t)]$ and the symmetric velocity $\hat{\mathbf{v}}(t) = [\mathbf{x}(t+\Delta t) - \mathbf{x}(t-\Delta t)]/(2\Delta t)$ in Eq. (2) [31]. Similarly, we derive an unbiased estimator for the noise term, which is constructed using a linear combination of four-point increments [30].

Remarkably, these modifications result in a vastly improved inference performance in the presence of measurement error [Figs. 1(f)–1(j)]. Specifically, while the bias becomes dominant at an error magnitude $|\eta| \sim \sigma\Delta t^{3/2}$ in the standard estimators, the bias-corrected estimators only fail when the measurement error becomes comparable to the displacement in a single time-step, $|\eta| \sim v\Delta t$ [Fig. 1(j)] [30]. Thus, our method has a significantly larger range of validity extending up to the typical displacement in a single time-frame.

Nonlinear dynamics.—Since our method does not assume linearity, we can expand the projection basis to include higher order functions to capture the behavior of systems with nonlinear dynamics. As a canonical example, we study the stochastic Van der Pol oscillator $\dot{v} = \kappa(1-x^2)v - x + \sigma\xi$, a common model for a broad range of biological dynamical systems [32]. We simulate a short trajectory of this process, with added artificial measurement error [Fig. 2(a)]. Indeed, we find that ULI reliably infers the underlying phase-space flow [Fig. 2(b)]. This is not limited to one-dimensional systems, as shown by studying convergence of higher-dimensional oscillators [Fig. 2(c)]. Importantly, this good performance does not rely on using a polynomial basis to fit a polynomial field: employing a nonadapted basis, such as Fourier components, yields similarly good results [30].

To capture the Van der Pol dynamics, only the three basis functions $\{x, v, x^2v\}$ are required. But can these functions be identified directly from the data without prior knowledge of the underlying force field? To address this question, we introduce the concept of partial information. We can estimate the information contained in a finite trajectory as $\hat{I}_b(n_b) = (\tau/2)\hat{\sigma}^{-2}_{\mu\nu}\hat{F}_{\mu\alpha}\hat{F}_{\nu\alpha}$, where $\hat{F}_{\nu\alpha}$ are the projection coefficients onto the basis b with n_b basis functions [8]. To assess the importance of the nth basis function in the expansion, we calculate the amount of information it contributes:

$$\hat{I}_b^{(\text{partial})}(n) = \hat{I}_b(n) - \hat{I}_b(n-1), \tag{4}$$

which we term the partial information contributed by the basis function b_n. This approach successfully recovers the

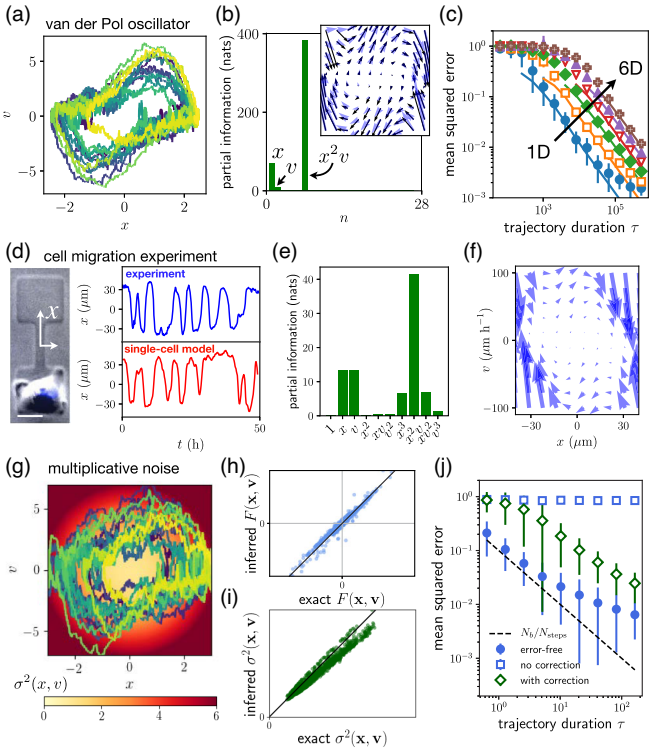

FIG. 2. Inferring nonlinear dynamics and multiplicative noise. (a) xv trajectory of the stochastic Van der Pol oscillator, $F(x,v) = \kappa(1-x^2)v - x$ with measurement error. (b) Partial information of the 28 basis functions of a sixth-order polynomial basis in natural information units (1 nat $= 1/\log 2$ bits), inferred from the trajectory in (a). Inset: Corresponding force field reconstruction. (c) Convergence of the inference error for the d-dimensional Van der Pol oscillator $F_\mu(\mathbf{x},\mathbf{v}) = \kappa_\mu(1-x_\mu^2)v_\mu - x_\mu$ (no summation, $1 \le \mu \le d$) with $d = 1,\ldots,6$, using a third-order polynomial basis. (d) Microscopy image of a migrating human breast cancer cell (MDA-MB-231) confined in a two-state micropattern (scale bar: 20 μm). Experimental trajectory of the cell nucleus position, recorded at a time interval $\Delta t = 10$ min (blue), and simulated trajectory using the inferred model (red). (e) Partial information for the experimental trajectory in (d), projected onto a third-order polynomial basis. (f) Deterministic flow field inferred from the experimental trajectory in (d). (g) Trajectory of a Van der Pol oscillator with multiplicative noise $\sigma^2(x,v) = \sigma_0 + \sigma_x x^2 + \sigma_v v^2$ (colormap). (h),(i) Inferred versus exact components of the force and noise term, respectively, for the trajectory in (g). (j) Inference convergence of the multiplicative noise amplitude, using Eq. (3) without measurement error (circles), with measurement error (squares), and using the error-corrected estimator (diamonds). The error saturation at large τ is due to the finite time step. Dashed line: predicted error $\delta\widehat{\sigma^2}/\widehat{\sigma^2} \sim \sqrt{N_b \Delta t/\tau}$ [8].

relevant terms in large basis sets [inset, Fig. 2(b)]. Thus, the partial information provides a useful heuristic for detecting the relevant terms of the force field.

To illustrate that ULI is practical and data efficient, we apply it to experimental trajectories of cells migrating in two-state confinements [Fig. 2(d)]. Within their lifetime, these cells perform several transitions between the two states, resulting in relatively short trajectories. Previously, we inferred dynamical properties by averaging over a large ensemble of trajectories [13,33,34]. In contrast, with ULI, we can reliably infer the governing equation of motion from single cell trajectories. Here, $F(x,v)$ corresponds to the deterministic dynamics of the system, and not to a physical force. We employ the partial information to guide our basis selection: indeed, it recovers the intrinsic symmetry of the system, suggesting a symmetrized third order polynomial expansion is a suitable choice [Fig. 2(e)]. Using this expansion, we infer the deterministic flow field of the system [Fig. 2(f)], which predicts trajectories similar to the experimental ones [Fig. 2(d)]. Importantly, the inferred model is self-consistent: reinferring from short simulated trajectories yields a similar model [30]. Using ULI, we can thus perform inference on small data sets, enabling "single-cell profiling," which could provide a useful tool to characterize cell-to-cell variability [34,35].

To demonstrate the broad applicability of our approach, we evaluate its performance in the presence of multiplicative noise amplitudes $\sigma_{\mu\nu}(\mathbf{x},\mathbf{v})$, which occur in a range of complex systems [13,14,36]. ULI accurately recovers the space- and velocity dependence of both the force and noise field, and the estimators converge to the exact values, even in the presence of measurement errors [Figs. 2(g)–2(j)]. To summarize, we have shown that ULI performs well on short trajectories of nonlinear data sets subject to measurement errors, and can accurately infer the spatial structure of multiplicative noise terms.

Collective systems.—A major challenge in stochastic inference is the treatment of interacting many-body systems. In recent years, trajectory data on active collective systems, such as collective cell migration [11,12] and animal groups [19–22,37], have become readily available. Previous approaches to such systems frequently focus on the study of correlations [19,38,39] or collision statistics [12,17,37], but no general method for inferring their underlying dynamics has been proposed. The collective behavior of these systems, ranging from disordered swarms [22] to ordered flocking [19], is determined by the interplay of active self-propulsion, cohesive and alignment interactions, and noise. Thus, disentangling these contributions could provide key insights into the physical laws governing active collective systems.

We consider a simple model for the dynamics of a 3D flock with Viscek-style alignment interactions [11,40–42],

$$\dot{\mathbf{v}}_i = \mathbf{p}_i + \sum_{j\neq i}[f(r_{ij})\mathbf{r}_{ij} + g(r_{ij})\mathbf{v}_{ij}] + \sigma\boldsymbol{\xi}_i, \qquad (5)$$

where $\mathbf{v}_i = \dot{\mathbf{r}}_i$, $\mathbf{r}_{ij} = \mathbf{r}_j - \mathbf{r}_i$, $\mathbf{v}_{ij} = \mathbf{v}_j - \mathbf{v}_i$, and $\mathbf{p}_i = \gamma(v_0^2 - |\mathbf{v}_i|^2)\mathbf{v}_i$ is a self-propulsion force acting along the direction of motion of each particle i. Here, f and g denote the strength of the cohesive and alignment interactions,

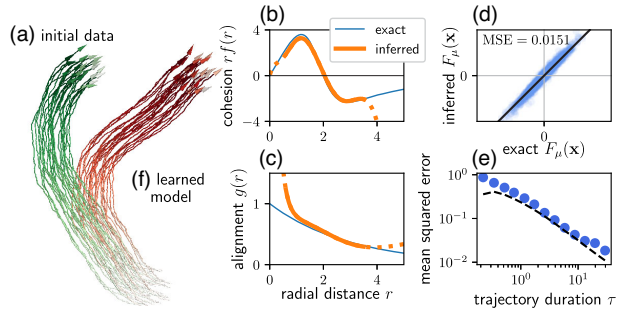

FIG. 3. Interacting flocks. (a) Trajectory (green) of $N = 27$ Viscek-like particles [Eq. (5)] in the flocking regime (1000 frames). We perform ULI on this trajectory using a translation-invariant basis of pair interaction and alignment terms, both fitted with $n = 8$ exponential kernels. (b) Exact (blue) and inferred (orange) cohesion $rf(r)$. Exact form includes short-range repulsion and long-range attraction, $f(r) = \epsilon_0[1 - (r/r_0)^3]/[(r/r_0)^6 + 1]$. Dotted inference dependence indicates distances not sampled by the initial data. (c) Exact and inferred alignment kernel $g(r)$. Exact form: $g(r) = \epsilon_1 \exp(-r/r_1)$. (d) Inferred versus exact components of the force field. (e) Convergence of the inferred force as a function of trajectory length. Dashed line is the predicted error $\delta\hat{F}^2/\hat{F}^2 \sim N_b/2\hat{I}_b$. (f) Simulated trajectory (red) employing the inferred force and noise, showing qualitatively similar flocking behavior.

respectively, as a function of interparticle distance r_{ij}. This model exhibits a diversity of behaviors, including flocking [Fig. 3(a)]. Intuitively, one might expect that ULI should fail dramatically in such a system: a 3D swarm of N particles has $6N$ degrees of freedom, and "curse of dimensionality" arguments make this problem seem intractable. However, by exploiting the particle exchange symmetry and radial symmetry of the interactions [30], we find that ULI accurately recovers the cohesion and alignment terms [Figs. 3(b) and 3(c)], and captures the full force field [Figs. 3(d) and 3(e)]. Furthermore, simulating the inferred model yields trajectories with high similarity to the input data [Fig. 3(f)]. This example illustrates the potential of ULI for inferring complex interactions from trajectories of stochastic many-body systems.

In summary, we demonstrate how to reliably infer the force and noise fields in complex underdamped stochastic systems. We show that the inevitable presence of discreteness and measurement errors result in systematic biases that have so far prohibited accurate inference. To circumvent these problems, we have rigorously derived unbiased estimators, providing an operational framework, Underdamped Langevin Inference, to infer underdamped stochastic dynamics [43]. Our method provides a new avenue to analyzing the dynamics of complex high-dimensional systems, such as assemblies of motile cells [11,12], active swarms [19,21,22,37], as well as nonequilibrium condensed matter systems [23,32,44].

We thank Alexandra Fink and Joachim Rädler for generously providing experimental cell trajectories. Funded by the Deutsche Forschungsgemeinschaft (DFG, German Research Foundation)—Project No. 201269156—SFB 1032 (Project No. B12). D. B. B. is supported by a DFG fellowship within the Graduate School of Quantitative Biosciences Munich (QBM) and by the Joachim Herz Stiftung. P. R. is supported by a Center for the Physics of Biological Function fellowship (National Science Foundation Grant No. PHY-1734030).

*c.broedersz@lmu.de
†These authors contributed equally.

[1] J. P. Crutchfield and B. McNamara, Complex Syst. **1**, 417 (1987), https://www.complex-systems.com/abstracts/v01_i03_a03/.
[2] B. C. Daniels and I. Nemenman, Nat. Commun. **6**, 8133 (2015).
[3] S. L. Brunton, J. L. Proctor, and J. N. Kutz, Proc. Natl. Acad. Sci. U.S.A. **113**, 3932 (2016).
[4] S. Siegert, R. Friedrich, and J. Peinke, Phys. Lett. A **243**, 275 (1998).
[5] M. Ragwitz and H. Kantz, Phys. Rev. Lett. **87**, 254501 (2001).
[6] M. E. Beheiry, M. Dahan, and J. B. Masson, Nat. Methods **12**, 594 (2015).
[7] L. P. García, J. D. Pérez, G. Volpe, A. V. Arzola, and G. Volpe, Nat. Commun. **9**, 5166 (2018).
[8] A. Frishman and P. Ronceray, Phys. Rev. X **10**, 021009 (2020).
[9] D. Selmeczi, S. Mosler, P. H. Hagedorn, N. B. Larsen, and H. Flyvbjerg, Biophys. J. **89**, 912 (2005).
[10] L. Li, E. C. Cox, and H. Flyvbjerg, Phys. Biol. **8**, 046006 (2011).
[11] N. Sepúlveda, L. Petitjean, O. Cochet, E. Grasland-Mongrain, P. Silberzan, and V. Hakim, PLoS Comput. Biol. **9**, e1002944 (2013).
[12] J. D'alessandro, A. P. Solon, Y. Hayakawa, C. Anjard, F. Detcheverry, J. P. Rieu, and C. Rivière, Nat. Phys. **13**, 999 (2017).
[13] D. B. Brückner, A. Fink, C. Schreiber, P. J. F. Röttgermann, J. O. Rädler, and C. P. Broedersz, Nat. Phys. **15**, 595 (2019).
[14] G. J. Stephens, B. Johnson-Kerner, W. Bialek, and W. S. Ryu, PLoS Comput. Biol. **4**, e1000028 (2008).
[15] G. J. Stephens, M. Bueno, D. Mesquita, W. S. Ryu, and W. Bialek, Proc. Natl. Acad. Sci. U.S.A. **108**, 7286 (2011).
[16] J. Gautrais, F. Ginelli, R. Fournier, S. Blanco, M. Soria, H. Chaté, and G. Theraulaz, PLoS Comput. Biol. **8**, e1002678 (2012).
[17] Y. Katz, K. Tunstrøm, C. C. Ioannou, C. Huepe, and I. D. Couzin, Proc. Natl. Acad. Sci. U.S.A. **108**, 18720 (2011).
[18] J. Jhawar, R. G. Morris, U. R. Amith-Kumar, M. Danny Raj, T. Rogers, H. Rajendran, and V. Guttal, Nat. Phys. **16**, 488 (2020).
[19] A. Cavagna, A. Cimarelli, I. Giardina, G. Parisi, R. Santagati, F. Stefanini, and M. Viale, Proc. Natl. Acad. Sci. U.S.A. **107**, 11865 (2010).

[20] A. Attanasi, A. Cavagna, L. Del Castello, I. Giardina, T. S. Grigera, A. Jelic, S. Melillo, L. Parisi, O. Pohl, E. Shen, and M. Viale, Nat. Phys. **10**, 691 (2014).
[21] J. Buhl, D. J. T. Sumpter, I. D. Couzin, J. J. Hale, E. Despland, E. R. Miller, and S. J. Simpson, Science **312**, 1402 (2006).
[22] A. Attanasi, A. Cavagna, L. Del Castello, I. Giardina, S. Melillo, L. Parisi, O. Pohl, B. Rossaro, E. Shen, E. Silvestri, and M. Viale, PLoS Comput. Biol. **10**, e1003697 (2014).
[23] G. Gogia and J. C. Burton, Phys. Rev. Lett **119**, 178004 (2017).
[24] A. E. Brown and B. de Bivort, Nat. Phys. **14**, 653 (2018).
[25] J. N. Pedersen, L. Li, C. Gradinaru, R. H. Austin, E. C. Cox, and H. Flyvbjerg, Phys. Rev. E **94**, 062401 (2016).
[26] F. Ferretti, V. Chardès, T. Mora, A. M. Walczak, and I. Giardina, Phys. Rev. X (to be published).
[27] B. Lehle and J. Peinke, Phys. Rev. E **91**, 062113 (2015).
[28] Since we interpret Eq. (1) in the Itô-sense, the inferred force field $F_\mu(\mathbf{x}, \mathbf{v})$ corresponds to this convention.
[29] P. Kloeden and E. Platen, *Numerical Solution of Stochastic Differential Equations* (Springer-Verlag, Berlin, Heidelberg, 1992).
[30] See the Supplemental Material at http://link.aps.org/supplemental/10.1103/PhysRevLett.125.058103 for detailed derivations of the correction terms and estimators.
[31] Note that, due to the change of definition of $\hat{\mathbf{v}}$, the prefactor of the correction term in Eq. (2) changes from $1/6$ to $1/2$.
[32] K. Kruse and F. Jülicher, Curr. Opin. Cell Biol. **17**, 20 (2005).
[33] A. Fink, D. B. Brückner, C. Schreiber, P. J. Röttgermann, C. P. Broedersz, and J. O. Rädler, Biophys. J. **118**, 552 (2020).
[34] D. B. Brückner, A. Fink, J. O. Rädler, and C. P. Broedersz, J. R. Soc. Interface **17**, 20190689 (2020).
[35] C. L. Vestergaard, J. N. Pedersen, K. I. Mortensen, and H. Flyvbjerg, Eur. Phys. J. Special Topics **224**, 1151 (2015).
[36] R. Friedrich, J. Peinke, and C. Renner, Phys. Rev. Lett. **84**, 5224 (2000).
[37] R. Lukeman, Y. X. Li, and L. Edelstein-Keshet, Proc. Natl. Acad. Sci. U.S.A. **107**, 12576 (2010).
[38] A. Cavagna, I. Giardina, and T. S. Grigera, Phys. Rep. **728**, 1 (2018).
[39] W. Bialek, A. Cavagna, I. Giardina, T. Mora, E. Silvestri, M. Viale, and A. M. Walczak, Proc. Natl. Acad. Sci. U.S.A. **109**, 4786 (2012).
[40] T. Vicsek, A. Czirok, E. Ben-Jacob, I. Cohen, and O. Shochet, Phys. Rev. Lett. **74**, 1226 (1995).
[41] G. Grégoire, H. Chaté, and Y. Tu, Physica (Amsterdam) **181D**, 157 (2003).
[42] H. Chaté, F. Ginelli, G. Grégoire, F. Peruani, and F. Raynaud, Eur. Phys. J. B **64**, 451 (2008).
[43] A readily usable PYTHON package to perform Underdamped Langevin Inference is available at https://github.com/ronceray/UnderdampedLangevinInference.
[44] M. Baldovin, A. Puglisi, and A. Vulpiani, PLoS One **14**, e0212135 (2019).